Back to the Basics – Event Analysis Using Symmetrical Components

Amanvir Sudan
Schweitzer Engineering Laboratories, Inc.

Presented at the
21st Annual Georgia Tech Fault and Disturbance Analysis Conference
Atlanta, Georgia
April 30–May 1, 2018

Originally presented at the
71st Annual Conference for Protective Relay Engineers, March 2018

Back to the Basics – Event Analysis Using Symmetrical Components

Amanvir Sudan, *Schweitzer Engineering Laboratories, Inc.*

***Abstract*—This paper highlights the use of symmetrical components for simplifying the analysis of events with uncommonly seen fault waveforms. The paper goes back to the roots and gives a brief refresher on symmetrical component theory. Then, three real-world events involving transformers are presented along with the relay event oscillography. A hypothesis is developed for each event to explain the waveforms, and then corresponding sequence networks are solved for phase currents to verify the hypothesis.**

I. Introduction

Symmetrical components are an indispensable tool for anybody in the field of power system protection, whether technician, engineer, or even operational personnel. They allow for substantially simplified short-circuit calculations, particularly for unbalanced faults. With the advent of microprocessor-based relays, they are now even used for protection purposes. Many protective elements, such as directional overcurrent (67), current unbalance (46), or ground overvoltage (59G) elements, rely on symmetrical components calculated in real time by digital relays. The new fault phase-selection logic used in digital relays is also based on symmetrical components [1]. Even some fault location algorithms employ symmetrical components, especially the negative-sequence components due to their immunity to system load flow and mutual coupling effects and due to their better homogeneity in negative-sequence impedance networks [2].

Traditionally, the core use of symmetrical components has been in studying and calculating unbalanced fault currents and voltages. Calculating these fault quantities is essential in sizing equipment, such as current transformers (CTs) and breakers, and in calculating protection settings. The theory of symmetrical components applied to fault calculations is well-known; it involves solving for symmetric (or sequence) quantities (namely, positive-, negative-, and zero-sequence quantities) and then using these sequence values to calculate unbalanced phase currents and voltages. However, this technique may not always yield exact solutions. The accuracy of this method is limited by the assumptions it makes. The method works on the premise of independent or decoupled positive-, negative-, and zero-sequence networks, which may not always be the case, especially with untransposed transmission lines [3]. In such cases, the alternative technique of phase analysis would be better-suited due to its holistic nature [4]. But despite the slight inaccuracy shortcoming, the symmetrical component method continues to offer great appeal due to its "close-enough" accuracy, widespread adoption, and even more importantly, its practical usability.

This paper highlights one such practical use of symmetrical components, and that is to aid in event analysis. Section III lists a simple approach for incorporating the theory of symmetrical components to help analyze event reports. The idea is to allow symmetrical components to be used as a tool to help understand fault oscillography, determine the root cause of an event, or simply allow someone to look at event report oscillography from a symmetrical component standpoint, for it may reveal useful information about the faulted power system. This method is performed with simple hand calculations using the already well-known symmetrical components theory, without any need for fault simulation software packages. If the technique presented here does not provide an explanation for the fault oscillography in an event report, more detailed methods such as those described in [5] should be tried.

This paper is divided into the following sections. We start with a refresher on the theory of symmetrical components in Section II. Next, an approach to event report analysis employing the use of symmetrical components is presented in Section III. The subsequent Section IV describes three real-world events and analyzes these events using symmetrical components.

II. Refresher on Symmetrical Components

The generalized theory of symmetrical components was devised by Charles L. Fortescue in 1913 while he was trying to study the effects of unbalanced currents on induction motor operation [6]. This method could be applied to a system with any N number of phases. C. F. Wagner and R. D. Evans applied this generalized theory of symmetrical components to study power system faults, and they introduced the concept of sequence networks. After that, E. L. Harder, W. A. Lewis, and Edith Clarke, among others, greatly simplified this method to the form that exists today.

What follows is a brief refresher on symmetrical components theory for readers familiar with the topic. There are numerous textbooks and references, such as [7] and [8], that cover the topic comprehensively for readers new to symmetrical components or those looking for additional details.

We start with the assumption this method makes. It considers the power system to be perfectly balanced under normal conditions. The only sources of unbalance in the power system are faults: shunt or series (open-circuit) faults.

The theory of symmetrical components states that any N set of unbalanced phasors can be broken down into n sets of symmetric phasors or components. In a three-phase system, these symmetrical components are zero-, positive-, and

negative-sequence components. For instance, A-phase, B-phase, and C-phase currents can be expressed as a linear combination of their respective zero-, positive-, and negative-sequence currents, as shown in (1). Similar relationships exist for the three phase voltages as well.

$$\begin{aligned} I_A &= I_{a0} + I_{a1} + I_{a2} \\ I_B &= I_{b0} + I_{b1} + I_{b2} \\ I_C &= I_{c0} + I_{c1} + I_{c2} \end{aligned} \tag{1}$$

As shown in Fig. 1, a set of positive-sequence currents is one with balanced currents matching the system phase rotation, which in this case is ABC. A set of negative-sequence currents is one with balanced currents but a phase rotation opposite to that of system phase rotation, or ACB in this case. A set of zero-sequence currents is one with all three currents having equal magnitudes and angles.

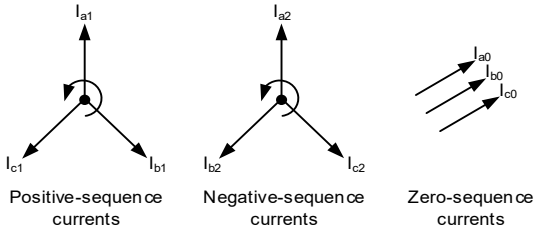

Fig. 1. Positive-, negative-, and zero-sequence currents of a system with ABC phase rotation

The equations in (1) can be further simplified and written in a matrix form, as shown in (2). They are covered widely in power system protection textbooks. The matrix relationship of (2) is valid for when the A-phase is selected as the base phase and ABC is the system phase rotation. Different matrix relationships hold when the B-phase and C-phase are the base phases or when the system phase rotation is ACB. (For instance, to calculate A-phase-to-B-phase fault currents using symmetrical components, the C-phase needs to be chosen as the base phase [8].)

$$\begin{bmatrix} I_A \\ I_B \\ I_C \end{bmatrix} = \begin{bmatrix} 1 & 1 & 1 \\ 1 & \alpha^2 & \alpha \\ 1 & \alpha & \alpha^2 \end{bmatrix} \begin{bmatrix} I_0 \\ I_1 \\ I_2 \end{bmatrix} \tag{2}$$

The α operator in the three-by-three matrix (called the A matrix) in (2) is a complex number with unity magnitude and a 120-degree angle. Further, using the inverse of the A matrix, we can derive (3) from (2), which enables the calculation of sequence currents from the given three-phase currents.

$$\begin{bmatrix} I_0 \\ I_1 \\ I_2 \end{bmatrix} = \frac{1}{3} \bullet \begin{bmatrix} 1 & 1 & 1 \\ 1 & \alpha & \alpha^2 \\ 1 & \alpha^2 & \alpha \end{bmatrix} \begin{bmatrix} I_A \\ I_B \\ I_C \end{bmatrix} \tag{3}$$

Each of these sequence currents has its own respective network in which it exists independently; these networks are the positive-sequence network, the negative-sequence network, and the zero-sequence network. Each of these networks is made up of sequence impedances corresponding to different elements in the power system, such as transformers, generators, and lines. The sequence impedance of a power system element is nothing but the impedance offered by the element to the flow of sequence currents when applied with respective sequence voltage sources.

These sequence impedances are determined in two ways. Depending on the power system element, the sequence impedance may either be provided directly by the manufacturer through testing and measurement as shown in Fig. 2, Fig. 3, and Fig. 4 (e.g., the transformer sequence impedance), or it may be calculated (e.g., the sequence impedances of the line [3]).

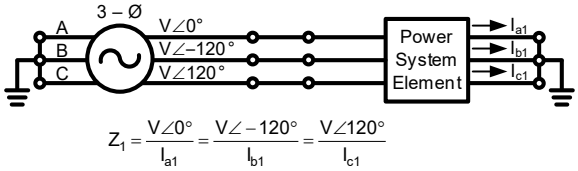

Fig. 2. Positive-sequence impedance measurement method

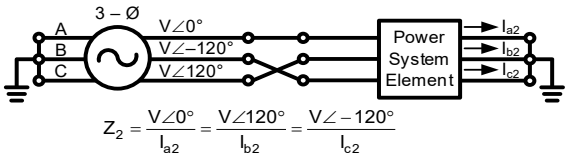

Fig. 3. Negative-sequence impedance measurement method

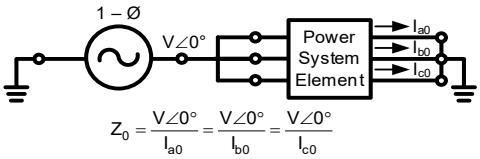

Fig. 4. Zero-sequence impedance measurement method

Fig. 5 shows the one-line diagram of an example power system, and Fig. 6, Fig. 7, and Fig. 8 show the corresponding positive-, negative-, and zero-sequence networks for this one-line diagram. There are a few key characteristics to note in these sequence networks. First, only the positive-sequence network contains the voltage source to represent the fact that the system generator produces only balanced phase voltages (or positive-sequence voltages) at its terminals and is not an inherent source of unbalanced voltages. Second, there are no discontinuities in the positive- and negative-sequence networks, as all the system elements shown in Fig. 2 allow for a continuous flow of positive- and negative-sequence currents.

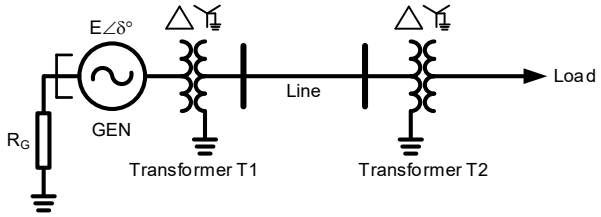

Fig. 5. One-line diagram of an example power system

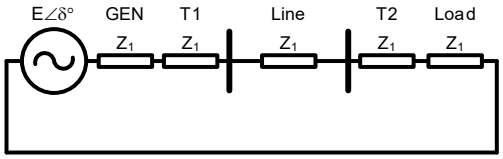

Fig. 6. Positive-sequence network of the example system

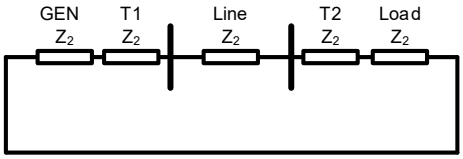

Fig. 7. Negative-sequence network of the example system

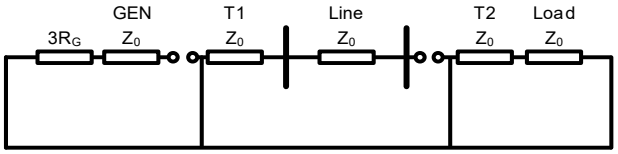

Fig. 8. Zero-sequence network of the example system

However, discontinuities can be observed in the zero-sequence network, and they are present at the point of the delta-connected transformer windings. The discontinuities exist because the delta windings do not allow zero-sequence currents to flow through; instead, they trap the zero-sequence currents. The zero-sequence currents of the three phases (since they are all equal) instead circulate within the triangular connection formed by the delta-connected windings. Hence, the zero-sequence impedance of a transformer is equal to the sum of the respective zero-sequence impedances of both the delta-connected and wye-connected windings.

Lastly, the grounding impedance R_G appears with a factor of three in the zero-sequence network. This can be understood as follows: if a zero-sequence voltage source were applied to this system, three zero-sequence currents (I_{a0}, I_{b0}, and I_{c0}, or simply I_0) would flow through R_G, and hence the overall voltage drop across the grounding impedance would be $R_G \bullet 3 \bullet I_0$. To show the effect of this voltage drop of $3I_0R_G$ in the sequence network of Fig. 8, where I_0 is the current flow, $3R_G$ is shown instead of R_G. A practical example of the zero-sequence voltage source would be an unbalanced fault involving the ground.

Next, to solve for different fault types, boundary conditions are determined at the fault point for voltages and currents in the phase domain. These phase boundary conditions are entered in (3) to derive the boundary relationships in the sequence domain. Then, to satisfy these sequence component relationships, the sequence networks are connected in either series or parallel at the fault point depending on the fault type, as shown in Fig. 9, Fig. 10, and Fig. 11.

The connected sequence networks are then reduced to solve for the sequence currents at the fault point using basic circuit theory. Once the sequence currents have been obtained, the phase currents at the fault location are calculated using the matrix relationship in (2).

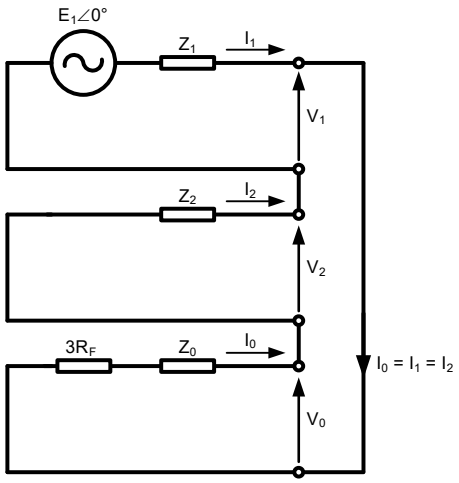

Fig. 9. Sequence network connection for a single-line-to-ground fault

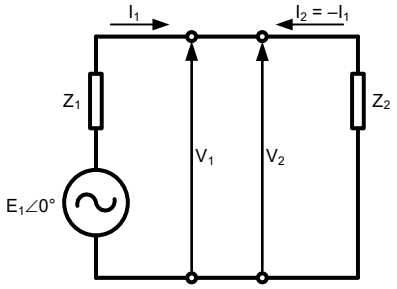

Fig. 10. Sequence network connection for a line-to-line fault

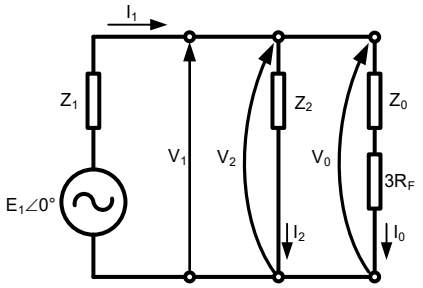

Fig. 11. Sequence network connection for a line-to-line-to-ground fault

III. Event Analysis With Symmetrical Components

Besides providing protection, microprocessor-based relays also allow for the capture and storage of fault oscillography and relay operation in event reports. These event reports contain valuable information, such as the phase voltages and currents before the fault, during the fault, and after the fault, and the duration of the event reports is typically user-settable. Along with these analog values, the event report also contains the statuses of various digital or binary bits. These binary bits are the indicators of the state of various function blocks and components in the relay, such as protective elements, input and output contacts, the breaker status, and so on. A binary bit could be in either an asserted state or a deasserted state. Additional

information, such as relay model, relay firmware, relay settings, and the time of the event report trigger, is also typically contained in the event report. The event report may also provide fault location if the relay supports that capability, its fault location setting is enabled, and it sees reliable fault data (fault currents and voltages). Further, each relay may handle the fault location calculation differently. Details on fault location calculations are typically available in the respective relay instruction manuals.

These event reports are literally the report cards of a protection scheme's performance, with the fault in the power system being the performance test. A fault is either going to result in a desired operation or an undesired operation by the protection scheme. A common case of an undesired operation is one where the protection scheme either trips when it should not or does not trip when it should. Event report analysis is essential in determining the root cause of any undesired operation or even for a corroboration of a desired operation.

There is no fixed methodology or technique to event report analysis, simply because each event is different. However, the following steps present a generalized approach to event report analysis. (Reference [9] comprehensively covers event report analysis with numerous examples.)

Step 1—Following any set company procedures and applicable regulatory compliance requirements, gather information on the event. This may include, but is not limited to, any available information about the system before and after the event (such as system operating conditions at the time of the trip), which breaker(s) opened, physical evidence of a fault, and so on. Based on this information, determine if a desired or an undesired operation by the protection scheme occurred.

Step 2—Gather all the relevant documentation, such as the system one-line diagram, the three-phase secondary connections drawing, the ac/dc schematic, and the nameplate data of the equipment involved in the event. Storing the instruction manual(s) for the relay(s) in service can be of great use in event analysis.

Step 3—Download the pertinent event report(s) from the relay(s). This includes the event report that captures the trip operation. The trigger time of this report should be close to or should match the actual known or recorded time of the trip.

It may also be useful (for plant- or system-wide analysis) or sometimes necessary (in the case of a failure-to-trip type of operation) to download the event reports from the nontripping relays whose report trigger times are close to the actual known time of the event. Collecting supervisory control and data acquisition (SCADA) logs and any station Dynamic Disturbance Recording (DDR) data could be helpful as well.

Finally, it is always best to download all the event report types for the pertinent event for the full duration of the event report length setting. These event report types include filtered, raw, Common Format for Transient Data Exchange (COMTRADE), and differential reports.

Step 4—In the event report timelines, note when the relay trips and identify which binary bit asserts exactly at that time. If the identified binary bit is programmed as one of the tripping conditions in the relay settings, then it is the one responsible for the trip.

Step 5—If it was a correct or desired operation, it could be validated by simply comparing the settings associated with the tripping binary bit with the measured analog quantity or the associated operate quantity (e.g., for a 51G operation, the ground current magnitude can be plotted against the ground overcurrent pickup setting).

Sometimes, the analog quantity may not be directly available in the event report. But, mathematical tools in event report software could be used to perform custom calculations and plot the analog quantity of interest. For example, the negative-sequence impedance can be calculated using the available voltage and current data and can be plotted to evaluate the operation of the respective directional element.

Step 6—For an undesired operation, plot and compare the analog or operate quantity with the relay element settings responsible for the trip. This step typically reveals either a need for a settings value adjustment (such as a pickup value or timer change) or a wiring error correction.

Also, pay attention to any errors in the logic settings of the relay; e.g., a missing pair of parentheses in the trip logic expression, missing supervisory logic in the trip equation, an incorrect Boolean expression, the wrong binary bit used, and so on. Proper commissioning of the whole protection scheme reduces the likelihood of such settings error-induced undesired operations [10].

Step 7—Additional steps may be necessary if the reason for the undesired operation has not been determined so far. This typically involves going further into detail with the tripping relay element logic diagram and algorithm, which are readily available in the relay instruction manuals.

Step 8—Look for binary bits that form a part of the tripping binary bit logic, referred to from here on as the "sub-binary bits." These sub-binary bits are either supervisory in nature (i.e., they must be asserted for the final tripping binary bit to assert, such as the torque control sub-binary bit), or they are blocking in nature (e.g., the reverse-looking mho element blocking in permissive overreaching transfer trip [POTT] and directional comparison blocking [DCB] schemes). In the event report, identify which supervisory or blocking sub-binary bit has unexpectedly asserted or deasserted and hence caused the undesired operation. Further, understand the purpose and logic behind the culprit sub-binary bit to make the adjustment in the relay settings that would have avoided such an undesired operation.

As a side note, combining multiple event reports from different relays is a great way to look at fault data from different (relay) locations in the power system, thus providing a system-wide view, which may be useful or sometimes even necessary in event analysis. The event reports can be easily combined if they are already time-synchronized, which is possible if the corresponding relays are time-synchronized to a Global Positioning System (GPS) clock. Otherwise, the event reports can be manually time-aligned.

The general approach presented can help identify the root cause of an undesired operation or simply help explain the relay processing and functioning that resulted in the desired operation. This approach focuses more on the relay operation based on the hard-coded relay logic, user-set relay settings, and whatever current and voltage waveforms the relay saw.

An additional approach based on symmetrical components is presented here and is meant to complement the previously described general approach to event analysis. This symmetrical component-based approach focuses more on the nature of the phase currents and voltages recorded in an event report. There is potentially a lot that could be learned about the power system and the faulted equipment from the phase currents and voltages captured in the event report by looking at them through a symmetrical components lens.

The symmetrical components-based approach can be used to accomplish the following:

- Explain the nature of fault waveforms that may not resemble classic fault waveforms.
- Estimate the fault location.
- Determine or verify the impedance values of various power system elements. (For example, [11] uses recorded sequence component values in event reports to validate transmission line impedances.)

We start by acknowledging the fact that the relays could be located far away from the actual fault location with multiple power system elements in between the relay and the fault location. Hence, the phase current and voltage waveforms the relay sees (or records in the event report) could essentially be different from the fault waveforms at the fault location (classic fault waveforms for line-to-line faults, line-to-ground faults, and so on).

To determine the phase currents (or voltages) at a location other than the fault location, we use the symmetrical component method of connecting the sequence networks (in either series or parallel) at the fault point. This approach is summarized in the following steps:

1. Using the system one-line diagram, build individual positive-, negative-, and zero-sequence network diagrams.
2. Connect the networks based on the known or expected fault location and fault type.
3. Using basic circuit theory, reduce the connected networks to calculate the sequence currents at the relay location.
4. Using (2), calculate the phase currents at the relay location and verify that they match the phase current waveforms recorded in the event report. (A similar procedure applies for voltages as well.)
5. If the calculated phase currents do not match the phase currents in the event report, change the expected fault location and fault type, and repeat this procedure starting from Step 2.

This approach does not even require system impedance data if we are trying to understand the non-classic fault waveforms. Rather, using the recorded voltages and currents, we can reverse-engineer the networks using the symmetrical components method and obtain a good estimate of the impedance values. Also, this approach is not meant to give precise answers for fault location, but is instead meant to provide a good enough estimate of where the fault could be and what type of fault it could be.

The idea is to provide a tool that is simple enough that it can be easily applied by anyone with basic knowledge of symmetrical components, using simple hand calculations.

IV. Case Studies

Three case studies are presented in this section, demonstrating the use of the symmetrical component-based approach in event analyses.

A. Case Study 1: Classic Phase-to-Phase Fault

Fig. 12 shows the one-line diagram of a system that experiences a phase-to-phase fault on one of its 12.47 kV feeders. The fault is successfully cleared by the inverse-time phase overcurrent (51P) relay on Feeder 2. Of course, this fault is also seen by the main breaker relay (51P) and the transformer differential (87T) relay.

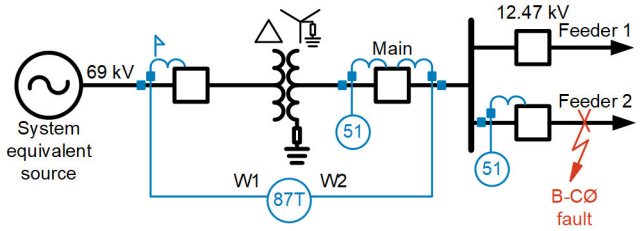

Fig. 12. System one-line diagram for Case Study 1

Fig. 13 shows the fault oscillography captured by the 87T relay. The 69 kV-side currents (Winding 1 [W1] current inputs) in the event report do not look like the phase-to-phase fault currents seen on the 12.47 kV side (Winding 2 [W2] current inputs). Here, IBW1 is almost twice that and opposite of IAW1 and ICW1. This current relationship occurs due to the delta-connected transformer windings on the 69 kV side, and it is easily proved using phase analysis. We can arrive at the same current relationship using the symmetrical components technique discussed in the previous section.

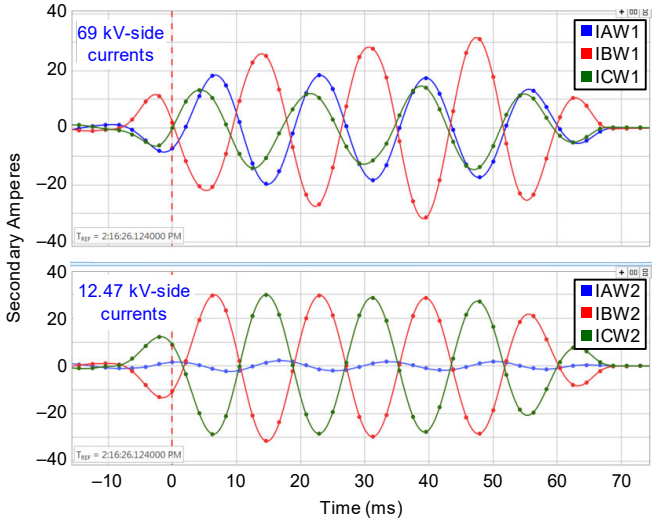

Fig. 13. 87T relay event report oscillography

We know that for a phase-to-phase fault, no zero-sequence quantities exist and the positive-sequence and negative-sequence networks are connected in parallel as shown in Fig. 10. The sequence network connection for the given system is shown in Fig. 12. In this network, I_1 and I_2 are the positive- and negative-sequence currents at the fault location, and they hold the relationship of $I_2 = -I_1$. The blue flags in Fig. 12 and Fig. 14 indicate the 69 kV-side currents measured by the W1 current inputs of the 87T relay. I_1' and I_2' are the positive- and negative-sequence currents at these flag locations. I_1' is the ±30-degree phase-shifted version of current I_1. The shift is ±30 degrees based on the transformer delta winding connections (DAB- or DAC-type delta connections) and the system phase rotation. After all, positive-sequence currents are nothing but balanced three-phase currents with ABC rotation; hence, they are phase-shifted by 30 degrees due to the delta winding connection just like any other balanced three-phase currents would be.

Similarly, I_2' is also the ±30-degree phase-shifted version of current I_2. However, the shift is opposite in nature to that of I_1'. This is because negative-sequence current phase rotation is the opposite of the system phase rotation, hence the phase shift induced in them is also opposite. (It is interesting to note from the oscillography in Fig. 13 that the W1 phase currents are not phase-shifted from the W2 phase currents.)

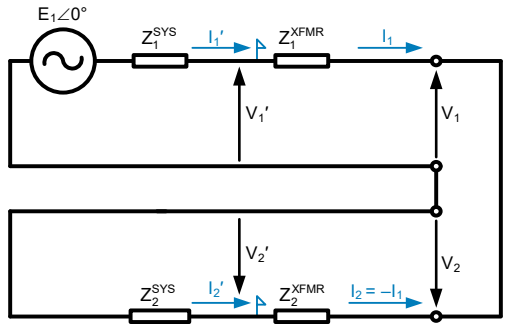

Fig. 14. Sequence network connection for phase-to-phase fault of Case Study 1

Assuming a DAB-type connection for the 69 kV delta windings and a system phase rotation of ABC, we can determine that the equations in (4) are true.

$$\begin{aligned} I_0 &= 0 \\ I_1' &= I_1 \bullet 1\angle 30^\circ \\ I_2' &= I_2 \bullet 1\angle -30^\circ \end{aligned} \tag{4}$$

Now that the positive- and negative-sequence currents have been determined at the point of interest, (2) can be used to determine the relationship between the phase currents at the relay location, as shown in the following equations.

From (2) and (4), we get (5).

$$I_A = 0 + I_1 \bullet 1\angle 30^\circ + I_2 \bullet 1\angle -30^\circ \tag{5}$$

Substituting $-I_1$ for I_2 in (5), we get (6).

$$\begin{aligned} I_A &= 0 + I_1 \bullet 1\angle 30^\circ - I_1 \bullet 1\angle -30^\circ \\ I_A &= I_1\angle 90^\circ \end{aligned} \tag{6}$$

Similarly, we can determine (7) and (8).

$$\begin{aligned} I_B &= 0 + \alpha^2 I_1 \bullet 1\angle 30^\circ - \alpha I_1 \bullet 1\angle -30^\circ \\ I_B &= I_1\angle 270^\circ - I_1\angle 90^\circ \\ I_B &= 2I_1\angle 270^\circ \end{aligned} \tag{7}$$

$$\begin{aligned} I_C &= 0 + \alpha I_1 \bullet 1\angle 30^\circ - \alpha^2 I_1 \bullet 1\angle -30^\circ \\ I_C &= I_1\angle 150^\circ - I_1\angle 210^\circ \\ I_C &= I_1\angle 90^\circ \end{aligned} \tag{8}$$

From these equations, we can see that the B-phase current is twice the A-phase and C-phase currents and that it flows in the opposite direction. This is exactly what we get using the phase analysis technique, and this is also what we observe in the oscillography in Fig. 13. Hence, symmetrical components provide an easy explanation and verification of the nature of the waveforms we see.

The Appendix shows the same technique applied to obtain voltages on the 69 kV side and to develop simple relationships among sequence voltages and currents on either side of the transformer in terms of the transformer sequence impedance.

The transformer impedance could also have been reverse-calculated had the sequence voltage and current data been available in the event reports from either side of the transformer. Or, the source impedance at the time of the fault could be reverse-estimated (including the transformer) using sequence voltages and currents captured in the main breaker relay event report.

B. Case Study 2: Brief In-Phase Currents

Fig. 15 shows a one-line diagram of a solar plant operating at 34.5 kV and connected to the electric grid at 500 kV through a three-winding, wye-wye connected transformer with a delta tertiary (500/34.5/13.8 kV). The plant operations report that the 87T relay generated an event report. It was nighttime when the event report was generated (hence, there was no solar generation at the time of the event, only consumption by the plant load). Additionally, no circuit breaker trips were reported.

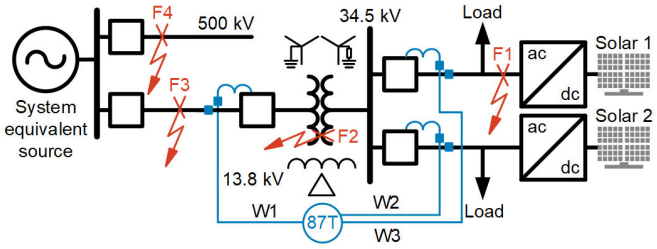

Fig. 15. System one-line diagram for Case Study 2

The event report oscillography from the 87T relay showing the 500 kV-side and the 34.5 kV-side currents is shown in Fig. 16. From this oscillography, it was observed that there was a three-cycle period where all three phase currents on the 500 kV side rose and went in phase and then resumed load flow. The 34.5 kV main breaker relays did not observe the in-phase currents phenomenon or any other fault activity. This was not the first time the relay generated such an event report. Plant operations wanted to know if this was a sign of anything failing in their transformer.

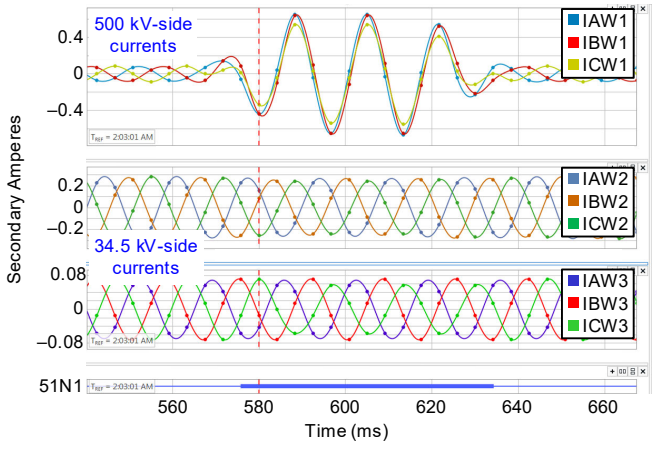

Fig. 16. Transformer 87T relay event report oscillography

The oscillography from the 34.5 kV feeder relay in Fig. 17, as expected, did not show any fault activity either.

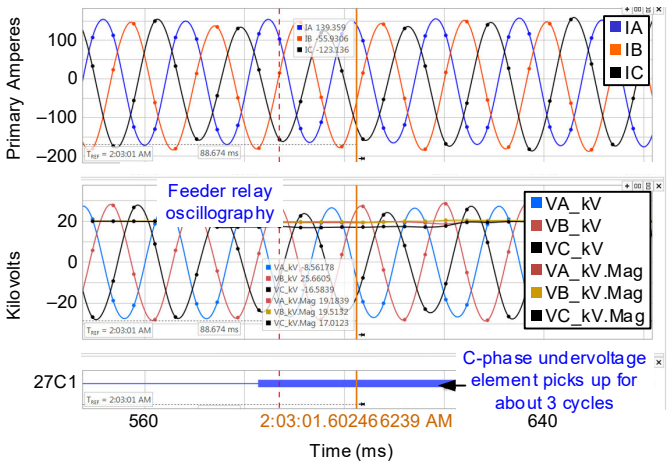

Fig. 17. Feeder relay event report oscillography

The first thing that stands out in the Fig. 16 event oscillography is that the high-voltage-side currents (IAW1, IBW1, and ICW1) are exactly equal in magnitude and angle. This hints at the presence of zero-sequence currents, which by definition flow equally in all three phases. The presence of zero-sequence current further hints at the involvement of the ground, as any fault involving ground contact generates zero-sequence currents. Also, the voltage is slightly perturbed only on the C-phase, as shown in Fig. 17, hence suggesting a likely ground fault on the C-phase. So, if it indeed is a C-phase-to-ground fault, where could it be?

There are only three possibilities: a fault outside the transformer on the 34.5 kV side (at location F1 in Fig. 15), a fault somewhere inside the transformer (at location F2), or a fault outside the transformer on the 500 kV side (at locations F3 or F4). The following subsections examine each of these possibilities using symmetrical components.

1) Possible Fault at F1

If the fault is external to the transformer at F1, the 87T relay 34.5 kV-side current inputs (Winding 2 [W2] and Winding 3 [W3]) should show some increase in current (at the same time the 500 kV-side current inputs are experiencing an increase in current). Or, if the fault is further downstream from 34.5 kV feeder relay, we should have also seen some fault activity in its respective event report (Fig. 17). But, neither the 87T relay W2 and W3 current inputs nor the feeder relays showed any fault activity. Hence, we can rule out the possibility of a fault at F1.

2) Possible Fault at F2

Here, the fault is assumed to be inside the transformer. From the Fig. 16 oscillography, we can see that there is strong zero-sequence current (as all the phase currents are in phase) and relatively negligible positive- and negative-sequence currents.

Fig. 18 shows the individual positive-, negative-, and zero-sequence networks for the given system. The solar generation is not shown in the figure, as this event occurred during nighttime and because solar inverters do not contribute significant and conventional currents for a fault. The load impedance is shown in all three networks. Given the substantially large impedance value of the load compared with the source and given the transformer impedance values, the impedance is typically ignored for simplicity. The internal fault point, F2, can be located anywhere inside the dashed box in the sequence networks, depending on where in the transformer the fault is. At this fault point, we connect the sequence networks in different fashions depending on the fault type. But, no matter how and where the F2 points in the positive-, negative-, and zero-sequence networks are connected, it is not possible for zero-sequence currents to flow through the faulted transformer without an accompanying flow of positive-sequence and negative-sequence currents. Given the fact that there is negligible positive-sequence current flow on the 500 kV side of the transformer as evident from the oscillography in Fig. 16 (predominately zero-sequence currents instead), we can deduce that a fault at F2 is unlikely.

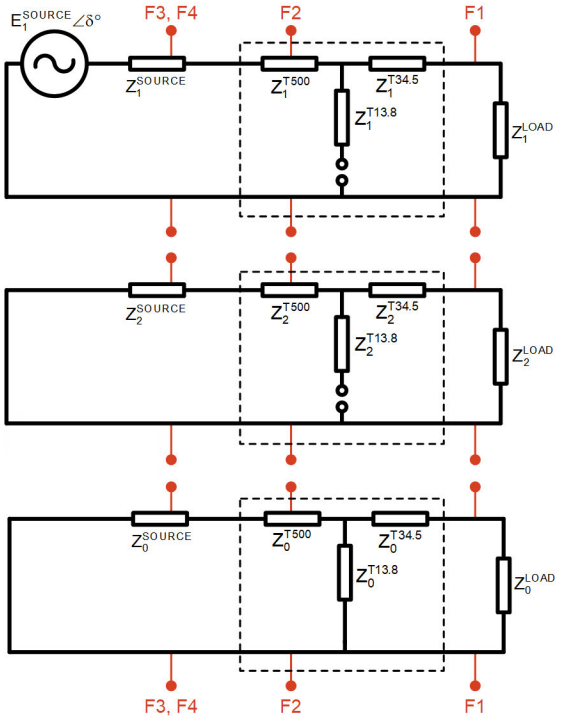

Fig. 18. Sequence networks showing the possible fault points for the system of Case Study 2

3) Possible Fault at F3

The only remaining possibility is an external fault in the 500 kV side of the system. Once again, assuming a ground fault is most likely, the sequence networks of Fig. 18 are connected as shown in Fig. 19.

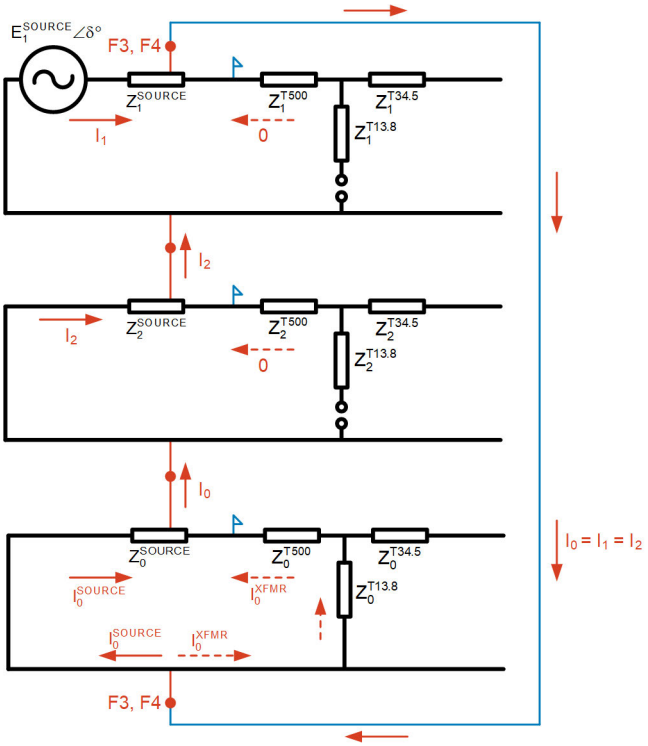

Fig. 19. Sequence network connection for external ground fault at 500 kV side for the system of Case Study 2

For an external 500 kV fault, there will not be any positive- or negative-sequence currents because of the open circuit in the delta tertiary in their respective sequence networks. The open circuit exists in these two networks because there is no way for positive-sequence and negative-sequence currents to circulate in an unloaded delta tertiary. However, since the zero-sequence currents in each phase winding (I_{a0}, I_{b0}, and I_{c0}) are equal to each other, they can easily circulate in the unloaded delta tertiary.

Referring to Fig. 19, we can infer that the 87T relay 500 kV-side current inputs (blue flags) are the only ones to see zero-sequence currents, confirming the oscillography observed in Fig. 17. (On a side note, the reason the 87T relay never operated even though there was a significant mismatch of measured current between the W1, W2, and W3 current inputs was because the current compensation settings were enabled in the relay. This effectively removed the large zero-sequence current of the W1 current input from the differential element calculations.)

Lastly, the fact that the fault waveforms only appear for three cycles and the voltage on all three phases is never lost indicates that this ground fault could not have been on the line feeding the transformer (F3), but rather that it was somewhere else in the system (e.g., at F4 on the adjacent line).

C. *Case Study 3: 87T Relay Undesired Operation*

The third event involves a three-winding, wye-wye connected transformer with a delta tertiary (230/34.5/13.8 kV) in another solar site application. This time, the event was an external fault on the 34.5 kV side. An A-phase-to-ground fault was reported at the splice junction box on one of the solar circuits. The one-line diagram showing the system and the fault location is shown in Fig. 20.

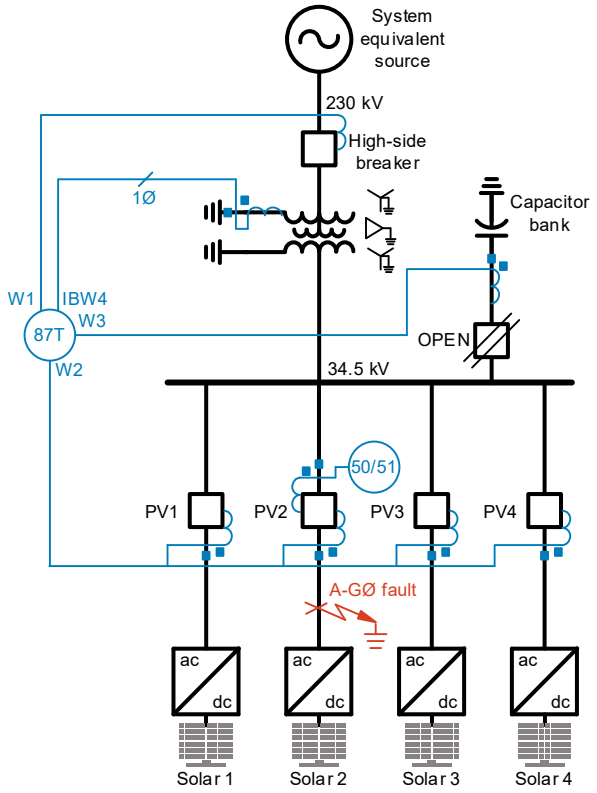

Fig. 20. System one-line diagram for Case Study 3

The faulted circuit (PV2) overcurrent relay sees the A-phase-to-ground fault current, as evident in its event report oscillography shown in Fig. 21.

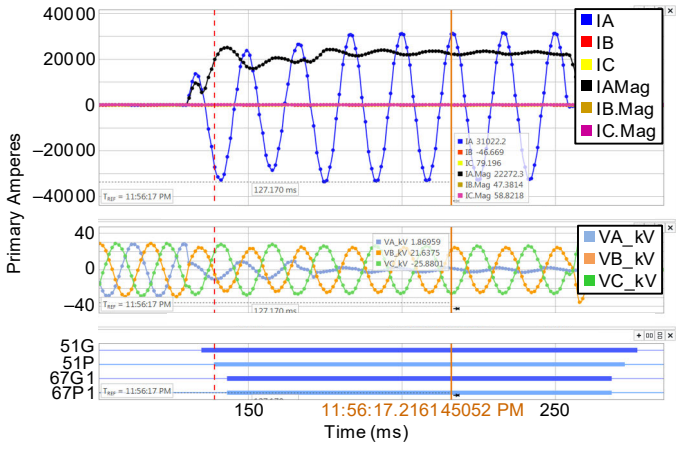

Fig. 21. Faulted feeder (PV2) relay event report oscillography

Before the relay could time out and trip, the transformer differential relay picked up for this external fault and tripped all the plant breakers through the associated lockout relay. Clearly, the 87T relay should not have operated for an external fault. The retrieved event report oscillography from the 87T relay showing the unfiltered currents is shown in Fig. 22.

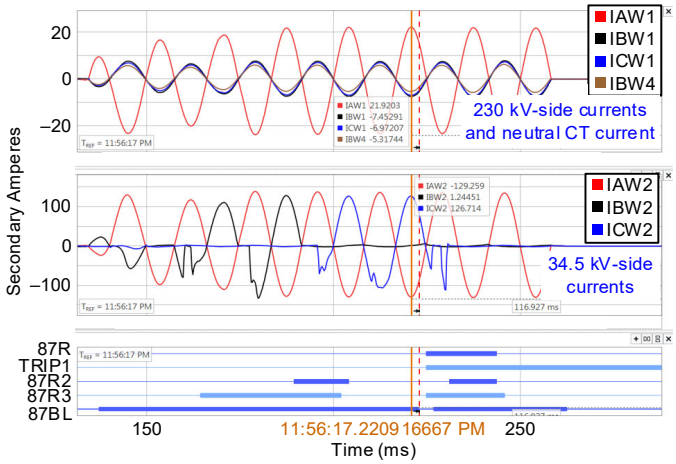

Fig. 22. 87T relay event report oscillography

The 87T relay W1 current inputs were connected to the 230 kV-side CT and the W2 current inputs were connected to the paralleled combination of all the feeder CTs, as shown in Fig. 20. The W3 current inputs were connected to CTs on the shunt capacitor bank branch. At the time of the event, the shunt capacitor bank was out of service. Lastly, the fourth current input W4 (IBW4) was connected to a single neutral CT in the grounded leg of the 230 kV wye-connected windings.

From the event report oscillography in Fig. 22, we can observe both the W1 and W2 current inputs registering fault activity on all the three phases. The IBW4 current input connected to the neutral CT also sees the fault current, as expected for a 34.5 kV-side ground fault.

Coming back to the 230 kV high-side currents (W1 current inputs), the B-phase and C-phase currents are exactly equal to each other and opposite of the A-phase current. The A-phase current is roughly three times the B-phase and C-phase currents. Interestingly, the A-phase current is roughly equal to the sum of the B-phase and C-phase currents and the neutral CT current (IBW4). (The symmetrical components analysis can once again be used to see if it can justify the current distribution on W1).

Next, the W2 current inputs also show fault signatures. The fault appears to be an “inconsistent” phase-to-phase fault. It shows as an A-phase-to-B-phase fault for the first few cycles, and then it switches to being an A-phase-to-C-phase fault. Throughout, the B-phase and C-phase current waveforms are marred by signal clipping, attenuation, and noise. These unusual signatures in IBW2 and ICW2 do not seem to translate over to the IBW1 and ICW1 currents on the other side of the transformer.

On the contrary, the PV2 circuit relay never captures any fault activity on the B-phase and C-phase, as evident from Fig. 21. One way this is possible is if there were simultaneous faults involving the B-phase and C-phase on other solar circuits; hence, only the 87T relay would see fault activity on all three phases, whereas the PV2 relay would only see its A-phase-to-ground fault. However, data captured from the other circuit relays refuted this possibility, as their respective

event reports contained no fault activity on the B-phase and C-phase. Lastly, there was no additional field evidence pointing toward B-phase and C-phase faults. Consequently, the possibility of simultaneous faults on other solar circuits can be ruled out. But then, how is it possible that the 87T relay shows fault activity on the B-phase and C-phase, but no corresponding fault activity is recorded by the PV2 relay? Perhaps because a fault involving the B-phase and C-phase actually never existed. The only other way the 87T relay would still show the B-phase and C-phase fault current activity is if an anomaly or discrepancy existed in the secondary circuits.

Sure enough, a subsequent field secondary wiring inspection revealed a missing connection. The missing connection was supposed to connect the 87T relay W2 current input non-dot polarity terminals to the ground and to the non-dot polarity of the paralleled CTs. The missing connection is shown as a dashed blue line in Fig. 23.

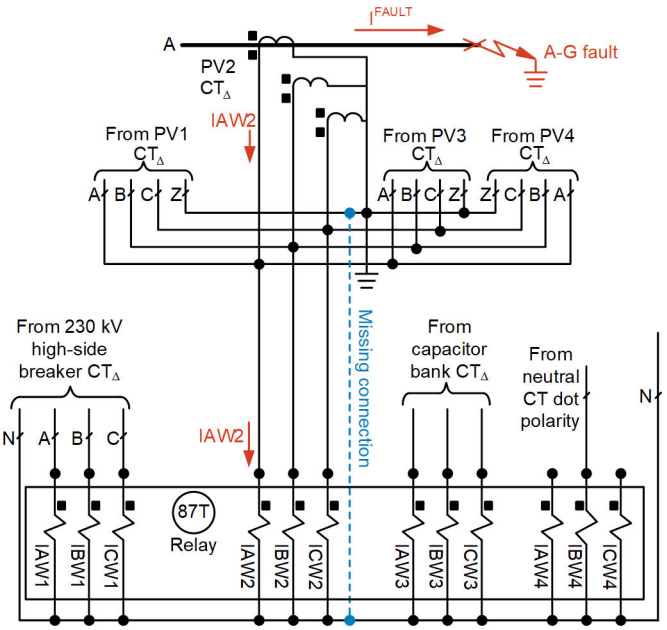

Fig. 23. Secondary connections of the 87T relay

Because of the missing connection, there is no direct return path from the relay W2 current inputs back to the paralleled CTs and the ground. If the current has to flow in the A-phase faulted circuit CT secondary, then it must somehow complete its current loop. From the connections shown in Fig. 23 and the oscillography of Fig. 22, it is clear that the IAW2 current returned intermittently via IBW2 and ICW2, hence completing the current loop (the nature of the randomness and clippings in IBW2 and ICW2 could be a topic of further research and investigation). This explains the 87T relay operation. The B-phase and C-phase currents are seen by the relay (due to a missing jumper) on the W2 side, but the corresponding B-phase and C-phase currents do not exist on the W1 side—a clear Kirchhoff current law violation. Fig. 24 shows the relay differential event report showing the operate current on the B-phase and C-phase to be above the slope times of the restraint current (the relay contained a dual-slope characteristic with slopes set at 25 and 60 percent). However, as expected, the 87 element corresponding to the A-phase never picks up.

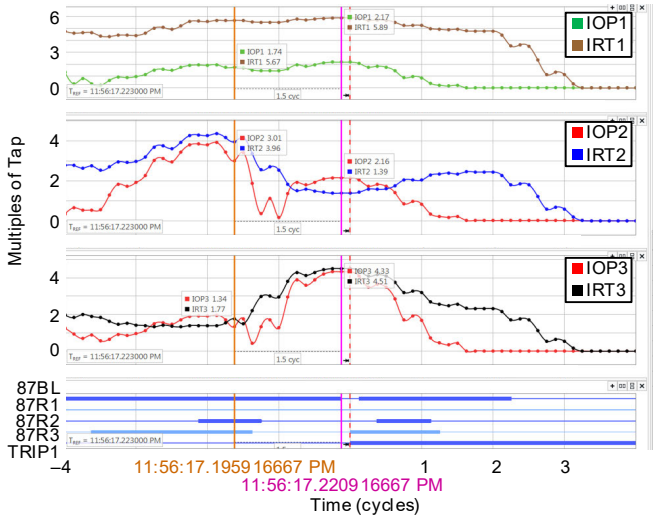

Fig. 24. Differential event report from the 87T relay

The 87 element is prevented from tripping initially because of harmonic blocking. The presence of harmonics due to unusual W2 B-phase and C-phase current waveforms (due to suspected CT saturation because of the missing connection) delays the differential operation through harmonic blocking until the harmonics subside.

With IBW2 and ICW2 put aside (present due to the missing return connection), the rest of the waveforms can once again be justified using symmetrical components. Fig. 25 shows the sequence network connections for this A-phase-to-ground fault.

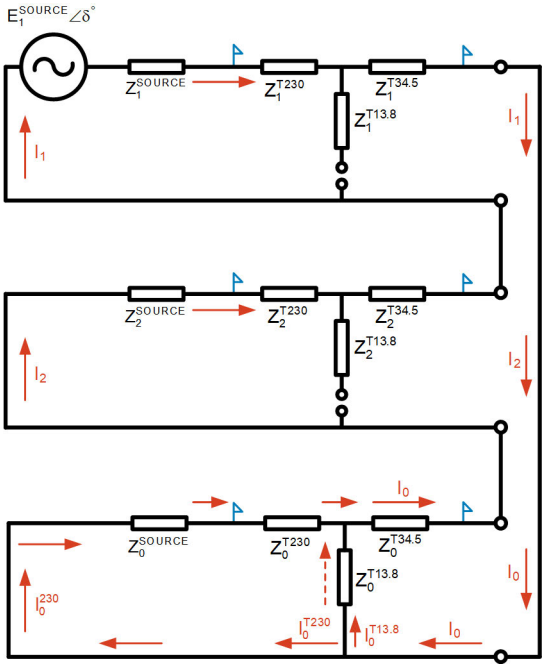

Fig. 25. A-phase-to-ground fault sequence network connection for the system of Case Study 3

From Fig. 25, we can see that the zero-sequence current (I_0) flowing to the 34.5 kV fault location is equal to the sum of the zero-sequence current circulating in the 13.8 kV delta-connected tertiary winding and the zero-sequence current flowing from the 230 kV side of the transformer. We can express this relationship as in (9).

$$I_0 = I_1 = I_2 = I_0^{T230} + I_0^{T13.8} \tag{9}$$

where:

$$I_0^{T230} = m \bullet I_0$$
$$m = \left(\frac{Z_0^{T13.8}}{Z_0^{T13.8} + Z_0^{T230}} \right) \tag{10}$$

Hence, we get (11).

$$I_0^{T13.8} = (1 - m) \bullet I_0 \tag{11}$$

Here, *m* is the ratio of the zero-sequence impedance of the 13.8 kV delta-connected tertiary winding to the total zero-sequence impedance of the source, the 230 kV wye-connected winding, and the 13.8 kV delta-connected winding.

To determine the phase current on the 230 kV side, we use the matrix equation of (2) as shown in (12).

$$\begin{bmatrix} IAW1 \\ IBW1 \\ ICW1 \end{bmatrix} = \begin{bmatrix} 1 & 1 & 1 \\ 1 & \alpha^2 & \alpha \\ 1 & \alpha & \alpha^2 \end{bmatrix} \begin{bmatrix} I_0^{T230} \\ I_1^{T230} \\ I_2^{T230} \end{bmatrix} \tag{12}$$

Using (9) and (10), the sequence currents of I_0^{T230}, I_1^{T230}, and I_2^{T230} in (12) can be expressed in terms of I_0, as shown in (13).

$$\begin{bmatrix} IAW1 \\ IBW1 \\ ICW1 \end{bmatrix} = \begin{bmatrix} 1 & 1 & 1 \\ 1 & \alpha^2 & \alpha \\ 1 & \alpha & \alpha^2 \end{bmatrix} \begin{bmatrix} m \bullet I_0 \\ I_0 \\ I_0 \end{bmatrix} \tag{13}$$

Expanding the matrix in (13) results in (14).

$$IAW1 = (m + 2) \bullet I_0$$
$$IBW1 = (m - 1) \bullet I_0 \tag{14}$$
$$ICW1 = (m - 1) \bullet I_0$$

Dividing IAW1 by IBW1 and ICW1, we get the relationship shown in (15).

$$IBW1 = ICW1 = \left(\frac{m-1}{m+2} \right) \bullet IAW1 \tag{15}$$

Equation (15) implies that for a 34.5 kV-side phase-to-ground fault, the current distribution on the 230 kV side of the transformer is a linear relationship dependent on the factor *m*.

The value of *m* could be anywhere between 0 and 1. The value is a scalar number if the system and transformer zero-sequence impedance are homogeneous. A value of 0 for *m* (which is the case with a nonexistent delta tertiary) results in IAW1 being twice that and opposite of IBW1 and ICW1. As the value of *m* increases, IAW1 grows larger in terms of IBW1 and ICW1. Or, we can look at the relative magnitudes of IAW1, IBW1, and ICW1 from the event report oscillography of Fig. 22 and reverse-calculate to obtain a rough estimate of *m*.

From the event report oscillography of Fig. 22, we can observe the values of IAW1, IBW1, and ICW1 shown in (16).

$$IAW1 = 21.9\angle 0°$$
$$IBW1 = 7.45\angle 180° \tag{16}$$
$$ICW1 = 6.97\angle 180°$$

From (16), we can determine that IAW1 is roughly three times IBW1 and ICW1, and it is opposite in nature. Putting this relationship into (15) results in a quarter of unity value for *m*.

$$\Rightarrow \frac{m+2}{m-1} = -3$$
$$\Rightarrow m = 0.25 \tag{17}$$

V. Conclusion

Event reports contain valuable data. They capture and store information about a fault and the relay response to the fault. Event report analysis is necessary for understanding a protection scheme operation. General event report analysis is based on a relay response to the fault according to the relay hard-coded logic and the user-set settings (numeric and logic). A complementary approach is presented in this paper to aid the general event report analysis method. This approach is centered on the nature of fault current and voltage oscillography observed in the event report and the anatomy of the faulted power system.

The approach involves drawing the sequence networks and connecting them based on the known or expected fault type and fault location. This allows for a holistic view of the faulted element and the rest of the system in the sequence domain. In this view, the fault may not always exist right next to the relay location. As a matter of fact, there may be multiple power system elements in between the relay location and the fault location. The presence of these power system elements, especially transformers consisting of delta-connected windings, alter the classic fault waveforms that exist at the fault location. Consequently, the far-located relay ends up seeing a deviation of the classic fault waveforms, which may not be readily understood in the captured event reports. But, by using basic circuit theory to solve for sequence currents and voltages (and hence, phase currents and voltages) at the relay location in the connected sequence networks, the peculiar nature of the observed non-classic fault waveforms can be explained.

Moreover, there are other advantages in drawing the sequence network connections. Doing so may provide additional insight into the characteristics of the faulted power system (e.g., determining the power system element impedance using the recorded sequence quantities data in the event reports, validating the known element impedance data, or building relationships between the observed fault oscillography and the power systems topology). Or, it may simply assist in determining the root cause of an event (e.g., determining the fault location as in Case Study 2).

VI. Appendix – Determining Unbalanced Phase Voltages Using Symmetrical Components on the Delta Winding Side of the Transformer of Case Study 1

Just as the phase currents on the delta side were determined by calculating I_1' and I_2' at the relay location in the sequence network connection of Fig. 14 (repeated here as Fig. 26), the phase voltages on the delta side can be similarly calculated by first obtaining V_1' and V_2' at the relay location.

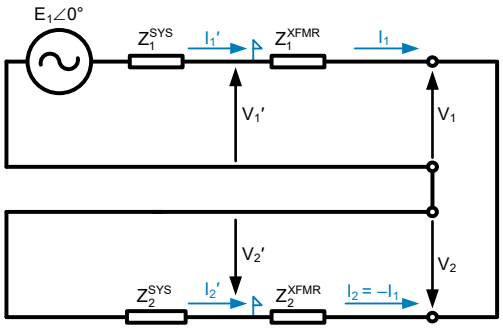

Fig. 26. Sequence network connection for phase-to-phase fault of Case Study 1

Just like the currents, the balanced voltages on the delta side are also phase-shifted by 30 degrees. As before, assuming the 69 kV delta windings of the transformer are connected in a DAB fashion, and assuming an ABC system phase rotation, we can infer that the positive-sequence voltages on the delta side will lead the wye-side positive-sequence voltages by 30 degrees. The reverse (a lagging phase shift of 30 degrees) is true for the negative-sequence voltages. Further, using Kirchhoff's voltage law in Fig. 26, we can write the relationships in (18) between V_1' and V_1 and between V_2' and V_2. (For brevity purposes, $1\angle 30$ degrees and $1\angle -30$ degrees have been directly appended in (18) to reflect the leading and lagging phase shifts resulting from the delta-connected windings.)

$$\begin{aligned} V_1' &= (V_1 + I_1 Z_1^{XFMR}) \bullet 1\angle 30° \\ V_2' &= (V_2 + I_2 Z_2^{XFMR}) \bullet 1\angle -30° \end{aligned} \tag{18}$$

Note the absence of the √3 factor in (18). In reality, balanced phase voltages (ABC or ACB phase rotation) on the delta side are √3 times greater than the respective balanced phase voltages on the wye side. The √3 factor does not appear in (18) because the equation is written in the per unit domain and the base voltage selection in per unit system calculations already incorporates the √3 factor. However, the phase shift does remain in the per unit system, hence the presence of ∠30° and ∠–30° in (18).

Next, substituting $I_2 = -I_1$ and $V_2 = V_1$ from Fig. 26 in (18) and given the fact that $Z_1^{XFMR} = Z_2^{XFMR}$ for three-phase transformers, we get (19).

$$\begin{aligned} V_1' &= (V_1 + I_1 Z_1^{XFMR}) \bullet 1\angle 30° \\ V_2' &= (V_1 - I_1 Z_1^{XFMR}) \bullet 1\angle -30° \end{aligned} \tag{19}$$

Once we know all three sequence voltages at the relay location (V_1' and V_2' from (19) and V_0' being 0 for a phase-to-phase fault), the phase voltages can be determined using (2), as shown in (20).

$$\begin{aligned} V_A &= V_0' + V_1' + V_2' \\ V_A &= 0 + (V_1 + I_1 Z_1^{XFMR}) \bullet 1\angle 30° + (V_1 - I_1 Z_1^{XFMR}) \\ &\quad \bullet 1\angle -30° \\ V_A &= \sqrt{3} V_1 \angle 0° + I_1 Z_1^{XFMR} \angle 90° \end{aligned} \tag{20}$$

Similarly, we can determine V_B and V_C as shown in (21) and (22).

$$\begin{aligned} V_B &= V_0' + \alpha^2 V_1' + \alpha V_2' \\ V_B &= 0 + (V_1 + I_1 Z_1^{XFMR}) \angle 270° + \\ &\quad (V_1 - I_1 Z_1^{XFMR}) \angle 90° \\ V_B &= 2 I_1 Z_1^{XFMR} \angle 270° \end{aligned} \tag{21}$$

$$\begin{aligned} V_C &= V_0' + \alpha V_1' + \alpha^2 V_2' \\ V_C &= 0 + (V_1 + I_1 Z_1^{XFMR}) \angle 150° + \\ &\quad (V_1 - I_1 Z_1^{XFMR}) \angle 210° \\ V_C &= \sqrt{3} V_1 \angle 180° + I_1 Z_1^{XFMR} \angle 90° \end{aligned} \tag{22}$$

These phase voltages and the currents from (6), (7), and (8) are summarized in (23), (24), and (25).

$$\begin{aligned} V_A &= \sqrt{3} V_1 \angle 0° + I_1 Z_1^{XFMR} \angle 90° \\ I_A &= I_1 \angle 90° \end{aligned} \tag{23}$$

$$\begin{aligned} V_B &= 2 I_1 Z_1^{XFMR} \angle 270° \\ I_B &= 2 I_1 \angle 180° \end{aligned} \tag{24}$$

$$\begin{aligned} V_C &= \sqrt{3} V_1 \angle 180° + I_1 Z_1^{XFMR} \angle 90° \\ I_C &= I_1 \angle 90° \end{aligned} \tag{25}$$

All of these expressions are in terms of the positive-sequence voltage (V_1) and current (I_1) at the fault location, which can be calculated from Fig. 26 as shown in (26).

$$V_1 = E_1 - I_1 (Z_1^{XFMR} + Z_1^{SYS}) \tag{26}$$

where:

$$I_1 = \frac{E_1}{Z_1^{XFMR} + Z_1^{SYS} + Z_2^{XFMR} + Z_2^{SYS}} \tag{27}$$

Assuming a purely inductive system for simplicity, we can draw the phasor diagram for Fig. 26 showing the voltages and currents on the delta side of the transformer for a B-phase-to-C-phase fault on the wye side of the transformer, as shown in Fig. 27.

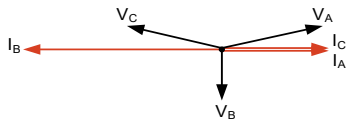

Fig. 27. Voltage and current phasors on the delta side for a B-phase-to-C-phase fault on the wye side of the transformer

VII. References

[1] D. Costello and K. Zimmerman, "Determining the Faulted Phase," proceedings of the 36th Annual Western Protective Relay Conference, Spokane, WA, October 2009.

[2] D. A. Tziouvaras, J. Roberts, and G. Benmouyal, "New Multi-Ended Fault Location Design for Two- or Three-Terminal Lines," proceedings of the CIGRE Study Committee B5 Colloquium, Florence, Italy, October 1999.

[3] E. O. Schweitzer, III, and S. E. Zocholl, "Introduction to Symmetrical Components" proceedings of the 30th Annual Western Protective Relay Conference, Spokane, WA, October 2003.

[4] S. Chase, S. Sawai, and A. Kathe, "Analyzing Faulted Transmission Lines: Phase Components as an Alternative to Symmetrical Components," proceedings of the 44th Annual Western Protective Relay Conference, Spokane, WA, October 2017.

[5] D. Tziouvaras, "Analysis of Complex Power System Faults and Operating Conditions," proceedings of the 35th Annual Western Protective Relay Conference, Spokane, WA, October 2008.

[6] C. L. Fortescue, "Method of Symmetrical Co-Ordinates Applied to the Solution of Polyphase Networks," *American Institute of Electrical Engineers*, Vol. 37, Issue 6, June 1918, pp. 629–716.

[7] J. L. Blackburn, *Protective Relaying: Principles and Applications*, 1st ed. Marcel Dekker, New York, NY, 1987.

[8] A. Amberg and A. Rangel, "Tutorial on Symmetrical Components Part 1: Examples," April 2013. Available: https://selinc.com.

[9] D. Costello, "Understanding and Analyzing Event Report Information," 54th Annual Conference for Protective Relay Engineers, College Station, TX, April 2001.

[10] K. Zimmerman and D. Costello, "Lessons Learned From Commissioning Protective Relaying Systems," proceedings of the 62nd Annual Conference for Protective Relay Engineers, College Station, TX, March 2009.

[11] A. Amberg, A. Rangel, and G. Smelich, "Validating Transmission Line Impedances Using Known Event Data," proceedings of the 65th Annual Conference for Protective Relay Engineers, College Station, TX, April 2012.

VIII. Biography

Amanvir Sudan received his bachelor of engineering degree in electrical and electronics engineering in 2011 from Panjab University in India. He then received his masters of science degree in electrical engineering, with a power system emphasis, in 2013 from Washington State University in the United States. Amanvir joined Schweitzer Engineering Laboratories, Inc. (SEL) in 2012 as an electrical engineering intern for the engineering services division of SEL where his focus was automation. Since January 2014, Amanvir has been working as an application engineer in protection in the sales and customer service division of SEL and supports SEL customers in the southwest region of the United States.

Previously presented at the 2018 Texas A&M Conference for Protective Relay Engineers.

20180301 • TP6848-01